PERFORMANCE CHARACTERISTICS AND MODELLING OF CEMENTITIOUS GROUTS FOR GEOTHERMAL HEAT PUMPS

Marita Allan and Aristodimos Philippacopoulos
Department of Applied Science, Brookhaven National Laboratory, Upton, New York 11973, USA

Key Words: geothermal heat pumps, grouts, thermal conductivity, heat transfer, thermal stresses, deformations.

ABSTRACT

The objectives of this work are to develop, characterize and model the behaviour of thermally conductive cementitious grouts for use with geothermal heat pump systems. The grouts have been tested for thermal, hydraulic, mechanical and other properties. The mean thermal conductivity of a grout formulation with 2.13 parts of sand to one part of cement by mass was 2.42 W/m.K. This is up to three times higher than bentonite grout and has a significant impact on lowering the overall thermal resistance. The mean coefficient of permeability for the same grout was 1.6×10^{-10} cm/s. When polyethylene pipes representing a U-loop heat exchanger were included in the system the mean coefficient of permeability increased to 1.9×10^{-7} cm/s due to imperfect interfacial bonding. Infiltration tests on grouted U-loops were conducted and the effect of circulating fluid temperature was measured to determine the efficacy of the grout for sealing boreholes. The infiltration rate remained of the order of 10^{-7} cm/s when fluid temperature was varied from 3 to 35°C demonstrating that the grout sealing performance was not significantly impacted. Finite element analysis was employed to evaluate the temperature distribution and the corresponding stresses and deformations developed within a grouted borehole as well as in the surrounding formation. The models developed incorporate all major components of the system (pipe/grout/formation). Heat transfer analysis was performed to evaluate the temperature distributions for the cooling and heating modes of operation. This task was followed by a thermal stress analysis.

1. INTRODUCTION

Boreholes used with closed loop vertical heat exchangers for geothermal heat pumps (GHPs) are grouted to meet performance and environmental requirements. The grouting material promotes heat transfer between the heat exchanger and the surrounding media and forms a hydraulic seal to protect aquifers from contamination. Traditionally, bentonite and neat cement (water plus cement) grouts have been used for this purpose despite the relatively low thermal conductivity and tendency to shrink and crack on loss of moisture. Furthermore, bonding to polyethylene pipes (U-loop/U-tube) is relatively poor for these materials. In response to these deficiencies research has been directed at development, testing and analysis of cementitious grouts that offer several significant benefits over conventional materials in terms of heat transfer, impermeability, dimensional stability, durability and cost effectiveness.

The numerical modelling component of the research involves analysis of several performance related issues. These include impact of contact resistance on heat transfer, effect of boundary conditions on temperature distribution within the grout and prediction of thermally induced stresses and deformations in the grout. A detailed two-dimensional finite element model of the ground heat exchanger has been developed which incorporates both pipes, grout and surrounding formation. The model permits a direct definition of heat sources and pertinent boundary conditions for the heat transfer and thermoelastic asymmetric problems. In addition, the model allows for simulation of air or water-filled gaps at the grout/U-loop interfaces which are considered in ongoing research. The thermal stresses and deformations developed in the ground heat exchanger have been analyzed for both heating and cooling modes of operation.

This paper describes the thermal and hydraulic properties of selected grout formulations and finite element analysis of heat transfer and thermal stresses. The hydraulic properties are important from an environmental perspective. Further details of the grout optimization and other properties can be found in Allan (1997), Allan and Philippacopoulos (1998) and Allan and Kavanaugh (1999).

2. MATERIALS

The basic cementitious grouts consisted of Type I (ordinary Portland) cement, silica sand between 75 and 1180 μm, bentonite, water and superplasticizer. The superplasticizer used was a liquid solution with 42% sodium naphthalene sulphonate by mass. This acts as a dispersant and improves grout pumpability. Variations on the basic mix included partial replacement of cement with fly ash or ground granulated blast furnace slag (BFS). The final mix represented a compromise between performance, cost, simplicity and compatibility with mixing equipment typically used in the US GHP industry. The sand/cement ratio was based on using one 42.6 kg bag of cement to two 45.3 kg bags of sand. The mix proportions and specific gravity of the superplasticized cement-sand grout (Mix 111) are presented in Table 1. Selected properties were measured on grouts with the same mix proportions except for 40% replacement of cement by mass with either ground granulated blast furnace slag (Mix 114) or fly ash (Mix 115).

3. EXPERIMENTAL PROCEDURES

3.1 Thermal Conductivity

Thermal conductivity was measured using the hot wire method with a Shotherm QTM-D2 Thermal Conductivity Meter. The grout was cast as blocks 75 mm x 125 mm x 25 mm. The blocks were cured in a water bath for 14 days prior to testing.

3.2 Coefficient of Permeability

Coefficient of permeability was measured on 102 mm diameter cylinders of grout and on grout cast around two lengths of 25.4 mm ID polyethylene pipe to represent a U-loop. The pipes were filled with wax to restrict permeation to either the grout or the grout/pipe interface. The first type of

test measured the hydraulic properties of bulk grout. Tests on grout cast around pipes incorporate any preferential flow at the interface between grout and polyethylene. Details of the testing procedure are given in Allan and Philippacopoulos (1998, 1999). A flexible wall triaxial cell permeameter was used. All specimens were cured for 28 days in water and vacuum saturated before testing at 21°C.

3.3 Infiltration Rate

Infiltration tests were performed to measure penetration of a head of water above grouted tubes containing a U-loop. At this stage only infiltration through the grout and at the grout/ U-loop interfaces has been considered. The test configuration was similar to that used by Edil et al. (1992) to study the sealing characteristics of different grouts for water wells. The experimental arrangement consisted of two PVC tubes each containing a U-loop. The tubes were 80 cm long and 102 mm internal diameter. Grout was tremied from the bottom up into the tubes using a 25.4 mm diameter tremie tube. A second PVC tube was glued to the top of each of the grouted tubes. The top tube was filled with water to give an initial head of 29 cm. A graduated burette was attached for viewing water elevation. The infiltration rate was calculated as the change in elevation with time.

The grout was allowed to cure for 28 days. Infiltration proceeded at room temperature for the first 68 days. Water at a temperature of 35°C was then circulated at a flow rate of 5.7 l/min through the U-loops for three weeks and infiltration rate was monitored. Following this, the circulating water temperature was decreased to 3°C for a further three weeks. The hot and cold temperatures of circulating water in the loops simulated operation of a heat pump in cooling and heating modes, respectively. It is recognized that operational temperatures may be outside the test range in some circumstances. The experiments enabled the effect of thermal expansion and contraction of the U-loop on infiltration rate to be determined. Due to the relatively short length of the U-loops, the inlet and outlet water temperatures were equal. Thus, the temperature gradient between loop legs that would occur in practice was not reproduced. If infiltration rate is controlled primarily by flow at the grout/U-loop interfaces and this, in turn, depends on differential thermal expansion and contraction of the system components then variation between experimental and field infiltration rates can be expected. It is predicted that the experimental infiltration rates will be lower than when hot water circulates and higher when cold water circulates since both pipes are expanding or contracting the same amount rather than differential deformations that occur with a temperature gradient.

Heat transfer between the U-loop and head of water resulted in temperature changes in the infiltrating water. The temperature of the water head was 33 and 8°C for the cooling and heating mode tests, respectively, and this must be taken into consideration when analyzing the results. In order to account for volume changes in the head of water associated with thermal effects, the changes in elevation were measured at equal temperatures so that the influence was constant.

4. EXPERIMENTAL RESULTS AND DISCUSSION

The average thermal conductivity of the Mix 111 grout when mixed under laboratory conditions was 2.42 W/m.K in the saturated state and 2.16 W/m.K when oven dried. This compares with 0.75 to 0.80 W/m.K for high solids bentonite and 0.80 to 0.87 W/m.K for neat cement grouts. Higher conductivity can be expected to enhance heat transfer and performance of the GHP. Furthermore, increased conductivity permits reduction of required bore length and, hence, decreased installation costs (Allan, 1997; Allan and Kavanaugh, 1999). Field mixed grout had an average thermal conductivity of 2.19 W/m.K in the saturated state. The lower conductivity may be due to lack of wet curing.

The results of the coefficient of permeability tests are given in Figure 1. The bulk Mix 111 grout had relatively low permeability coefficient of the order of 10^{-10} cm/s. Addition of fly ash to the grout increased permeability whereas blast furnace slag had a negligible effect for the curing period of 28 days. The coefficient of permeability increased significantly when polyethylene pipes were included in the system. However, the results were within the target order of 10^{-7} cm/s. The mean values were 1.9 x 10^{-7}, 2.4 x 10^{-7} and 5.3 x 10^{-7} cm/s for Mixes 111, 114 (slag-modified) and 115 (fly ash-modified), respectively. The increase is due to imperfect bonding between the grout and polyethylene. Incorporation of fly ash in the grout resulted in higher permeability coefficient and correlated with larger interfacial gaps. Although fly ash offers potential cost reductions, lower heat of hydration and improvement in durability, the negative impact on bonding is a concern for both environmental protection and heat transfer performance.

The mean infiltration rate data for the two grouted tubes is presented in Figure 2. The time interval for each data point was 7 days. There was no outflow for the system and, therefore, it was not possible to calculate falling head permeability. The graph shows that infiltration at ambient temperature decreases with time to steady state values. This is associated with ongoing cement hydration and consequent pore refinement. Circulation of hot or cold water caused temporary increases in mean infiltration rate and there was no consistent trend throughout the thermal cycles. Thus, it appears that there may be other effects controlling infiltration rate besides thermal expansion and contraction of the U-loop. The changes in temperature of the head of infiltrating water may have been influential due to corresponding changes in viscosity although this does not explain variations during a particular cycle. The infiltration rate remained of the order of 10^{-7} cm/s and the sealing capability of the Mix 111 grout was not significantly compromised by elevated or decreased temperature circulating fluid for the test conditions and duration.

It is recommended that the infiltration rate on full scale grouted boreholes be measured during heating and cooling modes in order to include the interfacial conditions between grout and surrounding formation and the effect of temperature gradients.

5. MODELLING APPROACHES

The steady state and transient heat transfer in vertical U-loop configurations of GHPs has been tackled both analytically and numerically. Analytical modelling is primarily based on line and cylindrical heating source solutions. Several works in this area are based on the early solutions by Carslaw and Jaeger (1940) and later on by Jaeger (1942). Cane and Forges (1991)

present a review of such models as they apply to problems related to heat pump configurations.

What made single source models applicable to U-tube thermal analysis was the concept of "equivalent diameter". Note that the presence of two legs in the U-loop generally requires non-symmetric solutions. Accordingly, Claesson and Dunard (1983) using superposition of two single sources to simulate the two pipes of the loop respectively extended earlier single source models. The use of the equivalent diameter is very attractive because it combines the two legs into one and therefore one can use available solutions from line or cylindrical source models thus avoiding complicated asymmetric solutions. Several studies, however, such as that by Mei and Baxter (1986), have shown that a large scatter in data exists. Lack of high confidence data has led the engineering community to doubt this modelling approach and find it not completely satisfactory. Specifically, there are concerns whether such an approach is valid over the range of parameters considered in GHP designs. Recently, the issue of the equivalent diameter was revisited by Gu and O'Neal (1998a). They point out that some of the discrepancies found before could be due to obtaining such values from steady-state solutions and then applying them to transient ones. They also conclude that the ratio of the equivalent diameter to the tube diameter can be two or greater.

Because simple analytical models were derived by assuming line and cylindrical sources in uniform spaces, they cannot take into account fundamental non-homogeneities existing in GHPs. Of primary importance is a material contrast between the grout and the surrounding formation. Even if one feels comfortable using an equivalent diameter, the impact of the grout on the heat transfer cannot be taken into account by such models. That is, the assumption that the heat transfer problem is symmetric may be acceptable in certain cases for simplicity. However, the assumption of homogeneous medium around the axis of the ground heat exchanger is not valid when the grout and the surrounding formation have distinct different material properties. Recognizing this difficulty, Gu and O'Neal (1995) developed an analytic solution for the transient heat transfer problem related to a cylindrical heat source in a nonhomogeneous medium. They used this solution later on (1998b) to evaluate grout effects on GHPs. It appears that the latter work represents the latest state-of-the-art in the domain of analytical modelling of GHP U-tubes. Obviously, none of the existing analytic models are non-symmetric per geometrical and thermal loading requirements of the problem. Thus, it is recommended that the latter requirements be considered in future research in the area of analytical modelling of U-tube ground heat exchangers. This can be done using appropriate Green's functions associated with explicit transient heat transfer solutions. Such models can be then employed with boundary element methods. Furthermore, they can provide essential tools to be used for benchmarking and verification of existing numerical modelling techniques.

A variety of numerical models were developed to overcome the limitations of existing analytic models. They are mostly of the finite difference type. There are very limited studies using finite element models available in the literature. Muraya (1994) used a two-dimensional finite element model to study the transient heat transfer in U-tube vertical heat exchangers of GHPs. Some benchmark problems were

utilized for verification purposes. They include both steady state as well as transient heat transfer solutions from single and dual source configurations. Thermal short circuiting between adjacent tubes was investigated using this modelling approach. Muraya (1994) extended 2D finite element heat transfer models to include moisture transport on the basis of the Phillip and de Vries (1957) theory and its extension by Hampton (1989). This combination resulted in non-linear transient heat and mass transfer finite element models. They are quite complex and their validity has not been adequately demonstrated. A more recent treatment of the moisture and heat transfer phenomena associated with the response of ground heat exchangers is given by Piechowski (1998)

The majority of existing numerical models of vertical ground heat exchangers of GHPs are based on finite difference techniques. Muraya (1994) and Gu (1995) give a review of such models in their theses. Since then, significant works in the area of finite difference modelling of vertical U-tube ground heat exchangers are those by Rottmayer et al. (1997), and Yavuzturk et al. (1998).

Rottmayer et al. (1997) modelled the system by a combination of cylindrical finite difference grids. They allow for heat transfer to occur radially and circumferentially in the ground. It is further assumed that no axial conduction occurs. The grid resembles 3D effects. A resistance network was considered for both the grout and the surrounding formation, which was used to set up the equations of heat conduction for the entire system. Computation of the transient heat transfer is reduced by 80% when two time steps are employed in the analysis.

The modelling approach by Yavuzturk et al. (1998) is based on an implicit finite volume formulation of the transient heat conduction in the two-dimensional space. The two legs of the U-tube can be simulated using this approach. Several assumptions were made to make the problem manageable. Among them, provisions were made so that the model simulates infinite medium conditions over the timeframe of the solution (constant far-field temperature). In addition, the grid was not sufficient to define directly the pipe elements and consequently the heating source (to simulate heat flux boundary conditions). Because the conduction process is referred to a single polar system it is geometrically difficult to define the input. Despite the number of assumptions made, Yavuzturk et al. (1998) have shown good correlation with temperature predictions from an analytical model. The model is used in conjunction with in-situ measurements of thermal conductivity (Austin et al., 1998).

In conclusion, both analytic and numerical heat transfer models applied to the U-tube ground heat exchangers require further development. In the analytical domain comprehensive exact solutions to the asymmetric 2D problem (including pipes, grout and formation) should be pursued so that available modelling techniques can be validated. In the numerical domain, the focus should be the finite element analysis, thus taking advantage of the significant developments in the last decade in this area.

6. HEAT TRANSFER AND THERMAL STRESSES

While much of the research in U-tube ground heat exchangers has focused on the thermal conductivity of the grout and on predictions of the temperature response, the corresponding

thermal deformation and stress fields have not been addressed. Their significance is reflected by the need of the designer to know the strength of the grout and its likelihood to develop thermal fractures.

Finite element analysis was performed to evaluate a) the heat transfer and b) the deformation and stress fields in the complete pipe/grout/formation system associated with U-tube ground heat exchangers. This system is modeled as a two-dimensional medium using 588 elements. Steady state conduction in the system was considered. In order to simulate the required infinite domain using finite models, a parametric investigation was made to define an appropriate far-field radius for the model. It was found that setting the latter at 10 ft produces comparatively good results. The alternative of using infinite elements to simulate infinite boundary conditions was also investigated. Such elements are attached radially to the exterior plane elements of the model. They are producing zero boundary conditions at infinity. A view of the overall FE model is shown in Figure 3 in which the ground heat exchanger portion (pipes plus grout) are depicted with only a part of the formation.

The thermal conductivities of the pipes, grout and formation were: 0.40, 2.42 and 1.73 W/m.K respectively. The entering and leaving water temperatures for the heating mode were: EWT=5°C, LWT=2°C. The corresponding values for the cooling mode were: EWT=30°C, LWT=36°C. These values were taken as worst case averages considering their variation with depth. Additional boundary conditions were imposed for the thermal stress analysis models so that they are adequately constrained. Plane strain conditions were used. Thermoelastic properties considered for each of the materials are: a) pipe: E=1.4 GPa, ν=0.45, α=2.16x10^{-4} m/m-$^{\circ}$C; b) grout: E=13.8 GPa, ν=0.21, α=1.65x10^{-5} m/m-$^{\circ}$C; and c) formation: E=2.0 to 5.5 GPa, ν=0.33, α=1.65x10^{-5} m/m-$^{\circ}$C (E=elastic modulus, ν=Poisson's ratio and α=coefficient of thermal expansion). The results were obtained with the ANSYS code.

The steady state temperature distribution is shown in Figure 4. Since the response inside the borehole is of primary interest, only results within the borehole are displayed. Similarly, thermal stresses for the cooling and heating mode of operations are shown in Figures 5 and 6 respectively. As expected, all results are symmetric with respect to the axis containing the two centers of the pipes. From Figure 4 it can be seen that the temperature distribution within the borehole for both heating and cooling modes of operation is reasonably smooth. A finer discretization was employed to model the grout. Additionally, two layers of elements were used to model the polyethylene pipes. It is because of such modelling provisions that relative smoothness in temperature results was obtained. A finer mesh does not seem to be required for the temperature solutions. However, for thermal stress solutions some additional refinement may be required for areas exhibiting stress concentrations. Specifically, for both modes of operation higher thermal stresses develop in the grout around the pipes. Comparison of Figures 5 and 6 with Figure 4 leads to the conclusion that the stress fields is consistent with those of the temperature. Stresses are especially higher in the grout near the axis of symmetry in the exterior area. This result is consistent with the physics of the problem. It is recommended that the values of the thermal stresses in these particular areas be evaluated using finer grids

consistent with standard practice with similar problems. Finally, the model allows for simulation of air or water-filled gaps at the pipe/grout interface. Also the contact between the grout and the formation is under investigation. Such interface conditions are expected to influence the heat transfer process in the pipe/grout/formation system and consequently the corresponding stresses and deformations.

7. CONCLUSIONS

Cementitious grouts can be tailored to meet property requirements for coupling polyethylene heat exchanger loops to surrounding ground in geothermal heat pump systems. Thermal conductivity can be improved by addition of silica sand to the grout. Coefficient of permeability and infiltration tests reveal that the grout acts as an effective sealant. Existing analytic and numerical modelling techniques for heat transfer in U-tube ground heat exchangers require further development to increase the reliability of current designs and system performance predictions. Presently, finite element modelling appears to be the most promising for predicting the response of ground heat exchangers to thermal loading.

ACKNOWLEDGEMENT

REFERENCES

Allan, M.L., (1997) *Thermal Conductivity of Cementitious Grouts for Geothermal Heat Pumps:* FY 1997 Progress Report, BNL 65129. 50 pp.

Allan, M.L. and Kavanaugh, S.P., (1999) Thermal conductivity of cementitious grouts and impact on heat exchanger length design for ground source heat pumps, *International Journal of HVAC&R Research*, Vol. 5, (2), pp. 87-98.

Allan, M.L. and Philippacopoulos, A.J., (1998) *Thermally Conductive Cementitious Grouts for Geothermal Heat Pumps:* FY 1998 Progress Report, BNL 66103. 78pp.

Allan, M.L. and Philippacopoulos, A.J., (1999) Groundwater protection issues with geothermal heat pumps, *Geothermal Resources Council Transactions,* Vol. 23, pp. 101-105.

Austin, W. A., Yavuzturk, C. and Spitler, J.D. (1998). Development of an in-situ system for measuring ground thermal properties. Submitted to *ASHRAE Trans.*

Cane, R.L. and Forgas D.A. (1991). Modeling of ground source heat pump performance. *ASHRAE Trans.*, Vol. 97, pp. 909-925.

Carslaw, H. S. and Jaegar, J. C. (1940). Some two-dimensional problems in conduction of heat circular geometry. *Proc. London Math. Soc.*, Vol. XLVI, pp. 361-388.

Claesson, J. and Dunard, A. (1983). Heat extraction from the ground by horizontal pipes- A mathematical analysis. *Swedish Council on Bldg. Res., D1,* Stockholm, Sweden.

Edil, T.B., Chang, M.M.K., Lan, L.T., and Riewe, T.V., (1992) Sealing characteristics of selected grouts for water wells, *Ground Water*, Vol. 30, (3), pp. 351-361.

Gu, Y. and O'Neal, D.L. (1998a). Development of an equivalent diameter expression for vertical U-tubes used in ground-coupled heat pumps. *ASHRAE Trans*., Vol. 102, pp. 1-9.

Gu, Y. and O'Neal, D.L. (1995). An analytic solution to transient heat conduction in a composite region with a cylindrical heat source. *J. Solar Energy Engrg., ASME*, Vol. 117, pp.242-248.

Gu, Y. and O'Neal, D.L. (1998b). Modeling the effect of backfills on U-tube ground coil performance. *ASHRAE Trans*., Vol. 104, pp. 1-10.

Gu, Y. (1995). Effect of backfill on the performance of a vertical U-tube ground-coupled heat pump. *Ph.D. Thesis*, Texas A&M University, College Station, Texas.

Hampton, D. (1989). Coupled heat and fluid flow in saturated-unsaturated compressible media. *Ph.D. Thesis*, Colorado State University, Ft. Collins, Co.

Jaeger, J. C. (1942). Radial heat flow in circular cylinders with a general boundary condition, *J. Roy. Soc. New South Wales*, Vol. 74, pp. 342-352.

Table 1. Mix Proportions of Cementitious Grouts

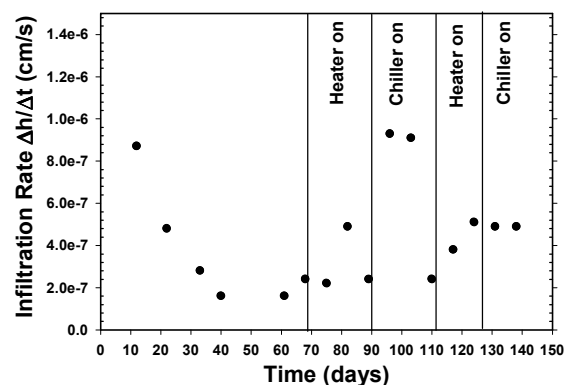|	Mix 111	Mix 114	Mix 115
Cement (kg/m³)	587.7	349.4	346.2
Fly ash (kg/m³)	0	0	230.8
Blast furnace slag (kg/m³)	0	233	0
Water (l/m³)	323.3	320.3	317.3
Sand (kg/m³)	1251.8	1240.5	1229
Bentonite (kg/m³)	6.5	6.4	6.3
Superplasticizer (l/m³)	8.8	8.7	8.7
Specific Gravity	2.18	2.16	2.14

Figure 2. Infiltration rate versus time for grouted tubes.

Mei, V. C. and Baxter, V. D. (1986). Performance of a ground coupled heat pump with multiple dissimilar U-tube coils in series. *ASHRAE Trans*., Vol. 92, pp. 30-42.

Muraya, N. K. (1994). Numerical modeling of the transient thermal interference of vertical U-tube heat exchangers. *Ph.D. Thesis*, Texas A&M University, College Station, Texas.

Piechowski, M. (1998). Heat and mass transfer model of a ground heat exchanger. *2nd Stockton Intl. Geoth. Conf.*

Phillip, J. R. and de Vries, D. A. (1957). Moisture movement in porous materials under temperature gradients. *Trans. Am. Geophys. AGU*, Vol. 38, pp. 222-232.

Rottmayer, S. P., Beckman, W. A. and Mitchell, J. W. (1997). Simulation of a single vertical U-tube ground heat exchanger in an infinite medium. *ASHRAE Trans*., Vol. 103(2), pp. 651-658.

Yavuzturk, C., Spitler, J.D. and Rees, S.J. (1998). A transient two-dimensional finite volume model for he simulation of vertical U-tube ground heat exchangers. Submitted to *ASHRAE Trans*.
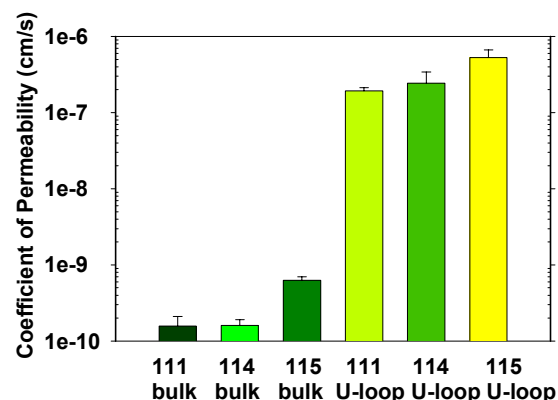
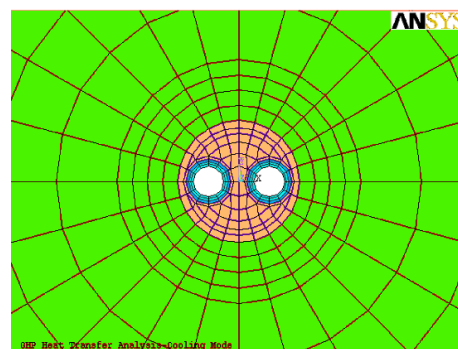Figure 1. Coefficient of permeability results for bulk grout and grouts cast around U-loop.
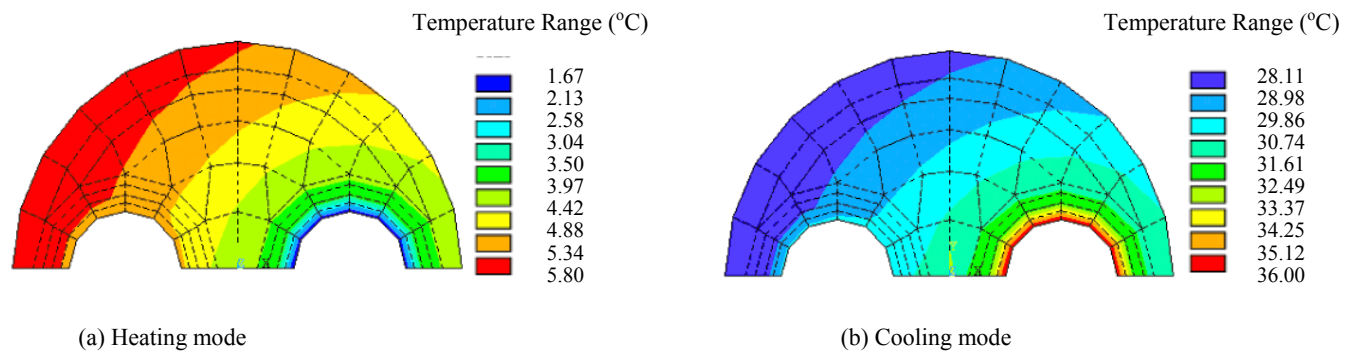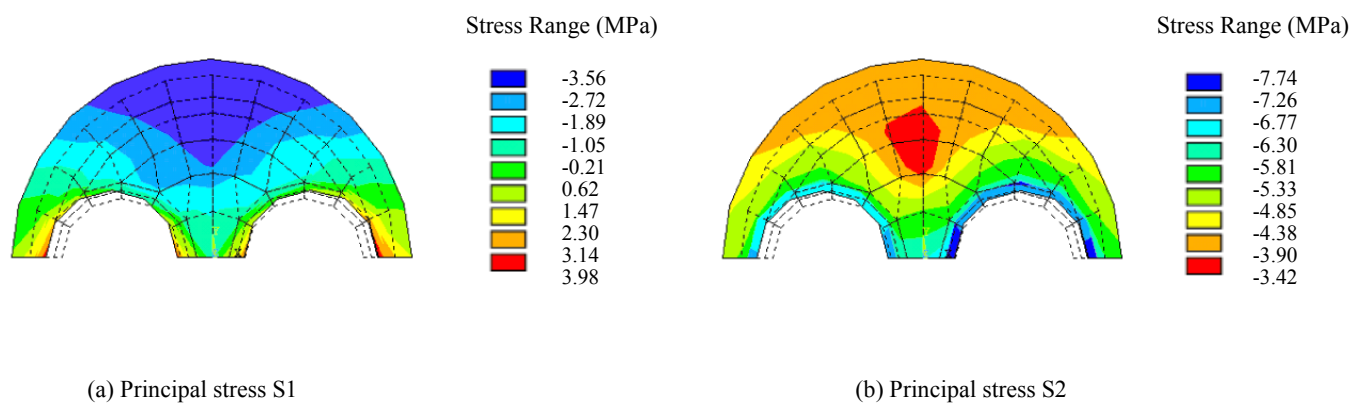

Figure 3. FEM detail near borehole

Temperature Range (°C)

■	1.67
■	2.13
■	2.58
■	3.04
■	3.50
■	3.97
■	4.42
■	4.88
■	5.34
■	5.80

Temperature Range (°C)

■	28.11
■	28.98
■	29.86
■	30.74
■	31.61
■	32.49
■	33.37
■	34.25
■	35.12
■	36.00

(a) Heating mode

(b) Cooling mode

Figure 4. Temperature distribution

Stress Range (MPa)

■	-3.56
■	-2.72
■	-1.89
■	-1.05
■	-0.21
■	0.62
■	1.47
■	2.30
■	3.14
■	3.98

Stress Range (MPa)

■	-7.74
■	-7.26
■	-6.77
■	-6.30
■	-5.81
■	-5.33
■	-4.85
■	-4.38
■	-3.90
■	-3.42

(a) Principal stress S1

(b) Principal stress S2

Figure 5. Thermal stresses for cooling mode of operation

Stress Range (MPa)

■	-7.36
■	-7.01
■	-6.67
■	-6.33
■	-5.99
■	-5.64
■	-5.31
■	-4.97
■	-4.62
■	-4.28

Stress Range (MPa)

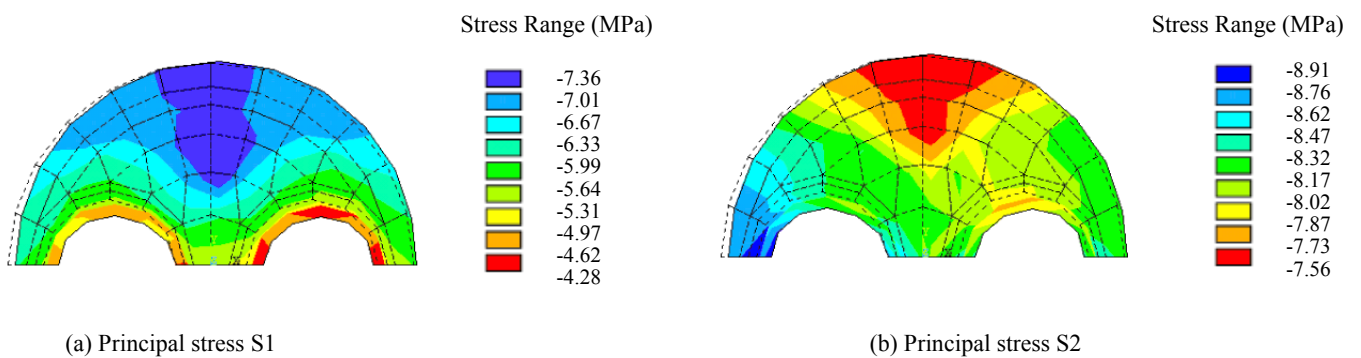|	
■	-8.91
■	-8.76
■	-8.62
■	-8.47
■	-8.32
■	-8.17
■	-8.02
■	-7.87
■	-7.73
■	-7.56

(a) Principal stress S1

(b) Principal stress S2

Figure 6. Thermal stresses for heating mode of operation